Ultrasound in Med. & Biol., Vol. 32, No. 5, pp. 759–767, 2006

0301-5629/06/$–see front matter

ELSEVIER

doi:10.1016/j.ultrasmedbio.2006.01.010

● *Original Contribution*

CAVITATION-ENHANCED ULTRASOUND THERMAL THERAPY BY COMBINED LOW- AND HIGH-FREQUENCY ULTRASOUND EXPOSURE

HAO-LI LIU,* WEN-SHIANG CHEN,[†‡] JHAO-SYONG CHEN,[§] TZU-CHING SHIH,[¶] YUNG-YAW CHEN,[‖] and WIN-LI LIN[‡§]

*Department of Electrical Engineering, Chang-Gung University, Taoyuan, Taiwan; [†]Department of Physical Medicine & Rehabilitation, National Taiwan University Hospital, Taipei, Taiwan; [‡]Division of Medical Engineering Research, National Health Research Institutes, Taipei, Taiwan; [§]Institute of Biomedical Engineering, National Taiwan University, Taipei, Taiwan; [¶]Institute of Medical Radiology Technology, China Medical University, Taichung, Taiwan; and [‖]Department of Electrical Engineering, National Taiwan University, Taipei, Taiwan

(*Received* 1 *July* 2005, *revised* 3 *January* 2006, *in final form* 17 *January* 2006)

Abstract—This paper demonstrates a novel approach for enhancing ultrasound-induced heating by the introduction of acoustic cavitation using simultaneous sonication with low- and high-frequency ultrasound. A spherical focused transducer (566 or 1155 kHz) was used to generate the thermal lesions, and a low-frequency planar transducer (40 or 28 kHz) was used to enhance the bubble activity. *Ex vivo* fresh porcine muscles were used as the target of ultrasound ablation. The emitted signals and the signals backscattered from the bubble activity were also recorded during the heating process by a PVDF-type needle hydrophone, and thermocouples were inserted to measure temperatures. Compared with the lesions formed by a single focused transducer, the size of the lesions generated by this approach were as much as 140% larger along the axial direction and 200% larger along the radial direction for combined 566- and 40-kHz sonication. They were 47% and 66% larger along the axial and radial directions, respectively, for combined 1155- and 28-kHz sonication. Cavitation activities enhanced by low-frequency ultrasound were confirmed by the presence of subharmonics in the spectrum and temperature increase as a result of increased tissue absorption. These observations imply that cavitation-enhanced lesions can be generated without reducing the penetration ability; they also show the advantage of producing larger and more uniform thermal lesions by multiple sonications. This technique provides an easy and effective way to achieve cavitation-enhanced heating, and may be useful for generating large and deep-seated thermal lesions. (E-mail: ychen@cc.ee.ntu.edu.tw)

Key Words: **Ultrasound thermal therapy, Cavitation-enhanced heating, Low-frequency ultrasound.**

INTRODUCTION

Ultrasound thermal therapy is an attractive and noninvasive method of tissue thermal therapy, and has increased in popularity throughout the past decade (Chapelon et al. 1999; Hynynen et al. 1993; Sanghvi and Hawes 1994; ter Haar 1995; Vaezy et al. 1998). Focused ultrasound in the therapeutic frequency range (0.5-3.5 MHz) offers good tissue penetration and can result in highly-focused energy deposition. The focused energy, after being absorbed by tissues for only a few seconds, can induce high temperatures (typically >60°C) and generate irreversible tissue necrosis at the target region while not damaging surrounding tissues (ter Haar 1995).

However, a major limitation of current ultrasound thermal therapy is the small lesion size and the resulting long treatment time (Fan and Hynynen 1996), and techniques to overcome this need to be developed. Acoustic cavitation, which is defined as the acoustically-induced activity of gas-filled cavities, is one such mechanism (Vallancien et al. 1992; Chapelon et al. 1999; Wu et al. 2001) that has potential to be clinically applied. Acoustic cavitation can be classified into stable and inertial cavitation (Flynn 1982). In stable cavitation, the radius of bubbles oscillates around an equilibrium size without collapsing over a considerable number of acoustic cycles (Barnett 1998; Tang et al. 2002). In inertial cavitation, bubbles grow rapidly within one or two acoustic cycles

Address correspondence to: Yung-Yaw Chen, Professor, Department of Electrical Engineering, National Taiwan University, BL-517, No. 1, Sec. 4, Roosevelt Road, Taipei 106, Taiwan. E-mail: ychen@cc.ee.ntu.edu.tw

before collapsing violently (Atchley and Crum 1988). Studies have shown that the occurrence of inertial cavitation may result in mechanical tissue destruction (Fry et al. 1970; Lele and Parker 1982; Vykhodtseva et al. 1995). The generated bubbles also act as ultrasound scatterers that reduce ultrasound penetration, and result in the formation of a tadpole-shaped lesion and a backward shift of the heating center (ter Haar 1995; Chen et al. 2003). Compared with tissue necrosis induced by a temperature build-up due to the absorption of ultrasonic energy, acoustic cavitation is more difficult to monitor, predict and control (Hynynen 1991; Barnett 1998; Meaney et al. 2000).

There is recent evidence that acoustic cavitation enhances the thermal heating process. Two attempts at cavitation-enhanced heating have been reported in focused ultrasound treatment. Sokka et al. (2003) used high-power short-pulse acoustic waves to stimulate gas bubbles before conventional continuous-wave exposure, with both stimuli provided by the same focused transducer. Their experiments showed that the generated thermal lesions become slightly rounder and shallower, with the lesion volume enlarged two- to threefold. Tran et al. (2003) showed that adding an ultrasound contrast agent into tissues can greatly reduce the intensity threshold as well as the heating duration required to induce a similar amount of tissue damage. Cavitation-enhanced heating was also observed in transparent tissue phantoms by Chen et al. (2003). The strategies used in these two approaches both relate to manipulating the cavitation threshold: the first increases the ultrasound intensity to stimulate the cavitation effect, and the second introduces artificial microbubbles into tissues to make it easier to induce cavitation.

This study employed a novel approach to induce cavitation-enhanced heating: low-frequency ultrasound exposure (28 to 40 kHz). Compared with ultrasound at megahertz frequencies, the pressure level to induce cavitation for kilohertz-frequency ultrasound is relatively low. (The threshold pressure to generate cavitation has been experimentally verified to nearly proportional to the ultrasound frequency (Flynn 1982; Hynynen 1991).) Moreover, the attenuation for low-frequency ultrasound is low, and hence deeper tissue can be treated. The main approach for confirming the existence of cavitation activity in the present study was to observe the spectrum of backscattered signals. The development of lesions and their dimensions were compared with and without simultaneous exposure to low-frequency ultrasound. The feasibility of using this approach to enhance ultrasound heating in large-volume scanning was also tested.

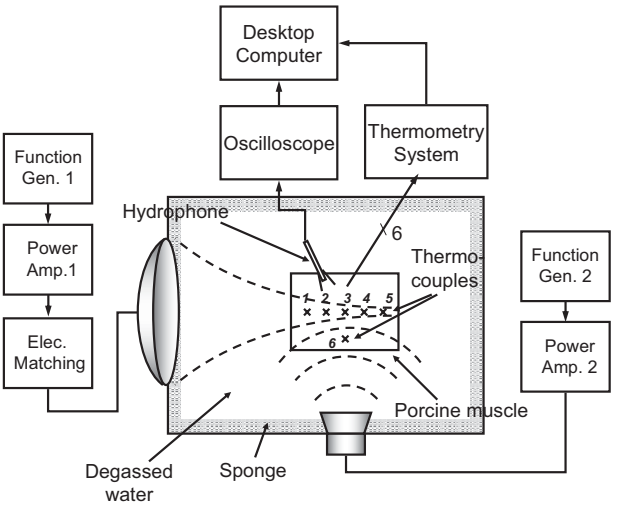

Fig. 1. Schematic diagram of the ultrasound sonication system.

MATERIAL AND METHODS

Experimental Setup

A block diagram of the experimental setup is shown in Fig. 1. To test the enhancement of the thermal effects by low-frequency ultrasound during the ultrasound thermal ablation without frequency specificity, low-frequency (28 or 40 kHz) and high-frequency (566 or 1155 kHz) ultrasound were both applied during the thermal ablation process. Two arrangements were used in this study. In arrangement 1, a 566-kHz PZT-4 spherical focused transducer (diameter = 10 cm, radius of curvature = 10 cm; components, Elecerom, Taoyuan, Taiwan) was combined with a 40-kHz planar transducer (K-Sonic Inc., Taiwan). In arrangement 2, a 1155-kHz PZT-4 spherical focused transducer (diameter = 10 cm, radius of curvature = 20 cm [Elecerom]) was combined with a 28-kHz planar transducer (K-Sonic Inc.). For each arrangement, the two ultrasound transducers were positioned orthogonally in an acrylic water tank with the axis of the planar crossing the geometric focus of the spherical. The two transducers were driven simultaneously using two arbitrary-function generators (33120A, Agilent, Palo Alto, CA; and DS345, Stanford Research Systems, Sunnyvale, CA) and two power amplifiers (150A250B and 150A100B, Amplifier Research, Souderton, PA), with both transducers operated in continuous-wave mode. The water tank was filled with deionized and degassed water at a temperature controlled to 25 ± 1°C. To prevent interference from scattered and reflected ultrasound waves, sponges were attached on four sides of the water tank. To detect the wideband signals during sonication, a calibrated polyvinylidene fluoride (PVDF)-type needle hydrophone (0.5 mm, calibrated range = 25 kHz to 20 MHz, Onda, Sunnyvale, CA) was used. To

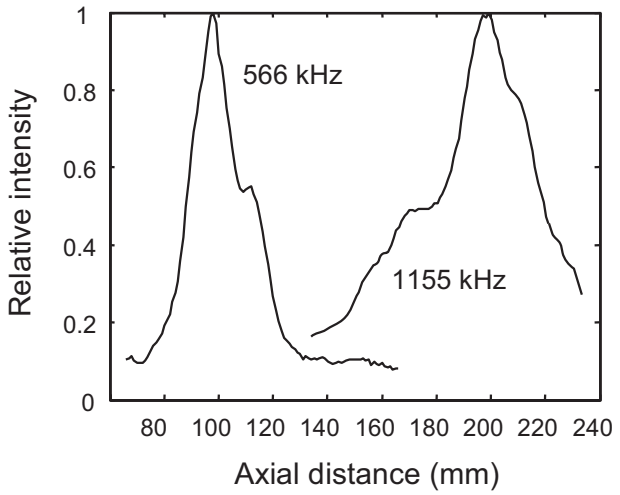

Fig. 2. Measured axial intensity distributions (in water) of the 566- and 1155-kHz focused ultrasound transducers.

restrict the received signals to those mostly coming from the focus, a plastic shield was mounted on the tip of the hydrophone. To avoid interference with the high-frequency focused ultrasound beam, the hydrophone was positioned out of the focal beam path of the 566- and 1155-kHz ultrasound. The hydrophone was also used to measure the pressure (and hence intensity) distribution of the 566- and 1155-kHz transducers along the radial and axial directions (measured by Broadsound Inc., Hsinchu, Taiwan; axial resolution = 0.25 mm, radial resolution = 0.5 mm). The measured axial intensities of the two focused ultrasound stimuli are shown in Fig. 2. The temperature increases were measured using multichannel thermometry system with J-type thermocouples (TC-2190, National Instruments, Austin, TX). Five thermocouples (thermocouples 1 to 5) were inserted to measure the temperature along the axis of the high-frequency ultrasound, with a 10-mm spacing. One thermocouple (thermocouple 6) was also placed 10 mm beneath the tissue surface on the side exposed to low-frequency ultrasound.

Experimental Procedures

The cavitation-enhanced ultrasound heating of tissues was assessed using freshly excised porcine muscle specimens in this study. All experiments were completed within 6 h of animal death. The tissue samples were placed under vacuum for approximately 10 min, and their surfaces were peeled to provide a smooth water–tissue interface. Tissue specimens were positioned so that the geometrical center of the focused 566- and 1155-kHz ultrasound was located 4 cm beneath the tissue surface.

Two sonication arrangements were made. In arrangement 1, the focused 566-kHz and planar 40-kHz ultrasound transducers were used. The peak intensity of the focused ultrasound transducer along the central axis was set to 260 W/cm^2, as calculated from an estimated tissue attenuation coefficient of 4.1 Np/m/MHz (Damianou and Hynynen 1993). This intensity was lower than the cavitation threshold according to the absence of subharmonics. For the 40-kHz planar transducer, the intensity at the target distance was set to 1.1 W/cm^2 (which was the upper limit of the device used). Sonication using 566-kHz transducer alone at the higher intensity of 450 W/cm^2 (which exceeds the cavitation threshold as verified by the presence of the 283-kHz subharmonic in the spectrum) was also conducted for comparison with combined 566- and 40-kHz sonication.

In arrangement 2, the focused 1155-kHz and planar 20-kHz ultrasound transducers were used. The peak intensity of the 1155-kHz ultrasound ranged from 95 to 125 W/cm^2 (estimated in the tissue), and the heating time ranged from 65 to 85 s. This intensity was also lower than the cavitation threshold, as confirmed by the absence of subharmonics in the spectrum. The ultrasound intensity for the 28-kHz transducer at the target distance was typically 2.3 W/cm^2 (upper limitation of the device used).

The intensities selected for the 566- and 1155-kHz ultrasound were aimed at producing similar rates of temperature increase, based on their similar specific absorption ratios in soft tissues—the tissue absorption ratio is approximately linearly dependent on frequency (Nyborg 1981). The applied low-frequency ultrasound alone (at 28 and 40 kHz) was also confirmed to induce acoustic cavitation by the presence of subharmonics (*i.e.*, 20- and 14-kHz components for 40- and 28-kHz ultrasound, respectively), which agrees with the reports of Suchkova et al. (1998) and Tang et al. (2002b).

During the exposures the two transducers were turned on simultaneously, and broadband signals were detected by a hydrophone and displayed on the screen of an oscilloscope (6030A, LeCory, Chestnut Ridge, NY). The data were also captured to a computer through a GPIB interface, and the spectra were calculated and analyzed using MatLab (Mathworks, Natick, MA). Frames were stored every 3 s, and the sampling rate of the oscilloscope was 20 MHz. Exposure times ranging from 20 to 100 s were used to produce thermal lesions of the order of centimeters in size.

Data Analysis

The specimens were dissected to evaluate the shapes and sizes of the induced lesions. To make the dissection process easier, the sonicated specimens were stored in a –20°C refrigerator for 30 min and partially thawed before dissection. The necrosed regions were

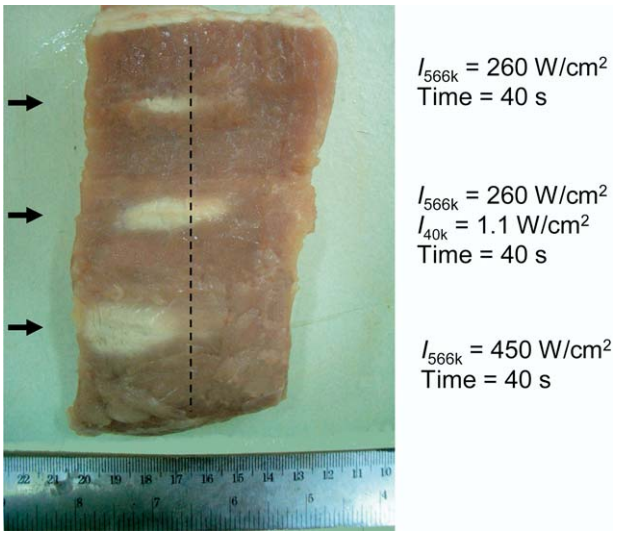

Fig. 3. Comparison of the thermal lesions generated in three conditions: 260-W/cm^2, 566-kHz ultrasound alone (top); combined 260-W/cm^2, 566-kHz and 1.1-W/cm^2, 40-kHz ultrasound (middle); and 450-W/cm^2, 566-kHz ultrasound alone (bottom). In all cases the exposure time was 40 s. Vertical dashed line indicates the focal depth of the 566-kHz transducer.

easily distinguishable based on their color: white confined regions compared with the surrounding fresh-red color. The lesion width and length were defined as the dimensions of the lesions along radial and axial directions. The mean ± SD values of the lesion length/width were used to perform statistical evaluations. Statistical significance was assessed using Student's t test, with a probability value of $p < 0.05$ considered to be significant.

RESULTS

Thermal Lesion Enhancement by Low-frequency Ultrasound

The enlargement of the thermal lesion by introducing low-frequency ultrasound exposures was investigated first. Figure 3 shows the typical thermal lesions generated from arrangement 1 (566 and 40 kHz). The top and middle lesions shown in Fig. 3 compares the thermal lesions produced with 566-kHz sonication alone and combined 566- and 40-kHz sonication. The intensity of the 566- and 40-kHz ultrasound was 260 and 1.1 W/cm^2, respectively, and the exposure time was 40 s. Under the same power intensity in focused ultrasound, the thermal lesion was larger for the combined ultrasound exposure. The bottom lesion in Fig. 3 was induced by 556-kHz ultrasound at an intensity of 450 W/cm^2, also for a sonication time of 40 s. The figure clearly shows that a tadpole-shaped lesion was generated. Moreover, the tadpole-shaped lesion tended to shift toward the transducer (bottom lesion in Fig. 3), whereas the enlarged thermal lesion (middle lesion) retained a symmetrical cigar shape centered close to the focal depth of the transducer.

The cavitation activity was verified by calculating the spectrum of the wide-band signal received by the PVDF-type needle hydrophone. Figure 4 compares the spectra related to the lesions shown in Fig. 3. Figure 4(b) shows that the first subharmonic (at 20 kHz) and other harmonics plus intermodulation products (at 60, 100, 140 kHz, *etc*.) of the 40-kHz ultrasound were both detected. Comparison of Fig. 4(c) with Fig. 4(a) shows that the first subharmonic for 566-kHz ultrasound was more pronounced when the ultrasound intensity was higher (*i.e.*, resulting in the acoustic cavitation threshold being exceeded).

The temperature elevations for the sonications in Fig. 3 along the axis of the 566-kHz ultrasound are shown in Fig. 5. A higher maximum temperature (by ~6°C, at ə = 3 cm) was observed for combined 566- and 40-kHz sonication (Fig. 5(b)) than for 566-kHz sonication alone (Fig. 5(a)). Figure 5 (c) indicates that the temperature was higher than 70°C for 566-kHz ultrasound at 450 W/cm^2, but this occurred at the proximal end (at ə = 1 cm). For comparison, Fig. 5(d) shows the temperature elevation induced by 40-kHz sonication alone. The temperature elevation was less than 1°C, which confirms that the low-frequency sonication alone did not result in significant temperature build-up in tissues. Also, the temperature elevation on the low-frequency sonication side (Thermocouple 6, 10 mm beneath the tissue surface) was less than 2°C during the entire sonication process (data not shown), confirming that

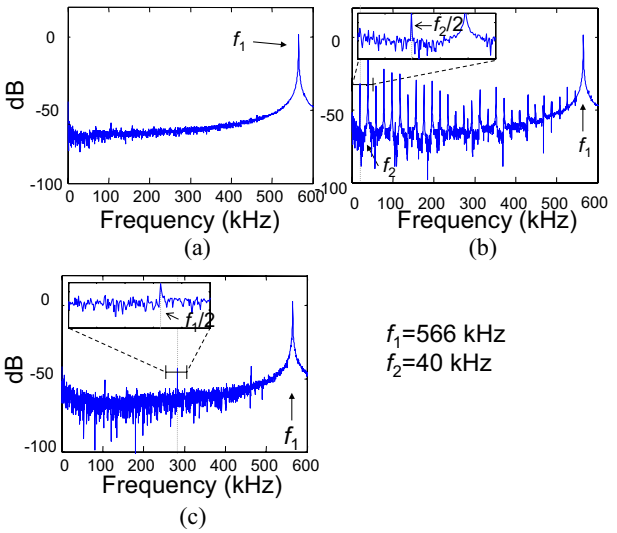

Fig. 4. Measured spectra corresponding to the sonications shown in Fig. 3, where f_1 and f_2 represent the center frequencies of the two transducers in arrangement 1 (566 and 40 kHz). The observed subharmonics are denoted as $f_1/2$ and $f_2/2$.

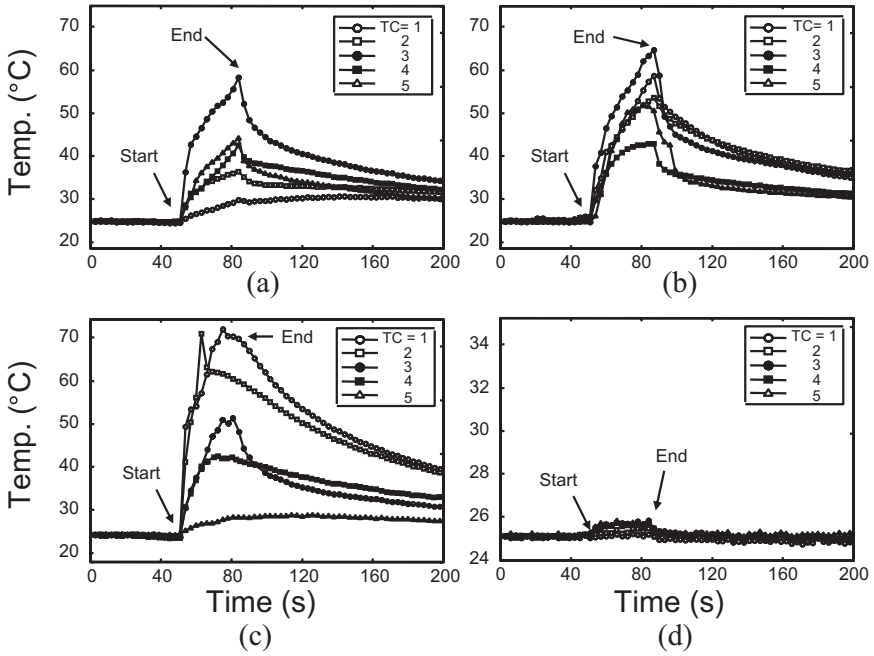

Fig. 5. Measured temperature evolutions along the axis of the 566-kHz ultrasound corresponding to the sonications shown in Fig. 3 ((a)-(c)), and during 40-kHz sonication alone (d).

thermal effects due to low-frequency sonication were negligible during the experiments.

A similar enlargement of the thermal lesion occurred for arrangement 2 (1155 and 28 kHz). Figure 6 compares the lengths and widths of the lesions produced between 1155-kHz ultrasound alone (95 W/cm^2) and combined 1155- and 28-kHz ultrasound (95 and 2.3 W/cm^2, respectively). The addition of the low-frequency ultrasound clearly increased the size of the thermal lesions induced.

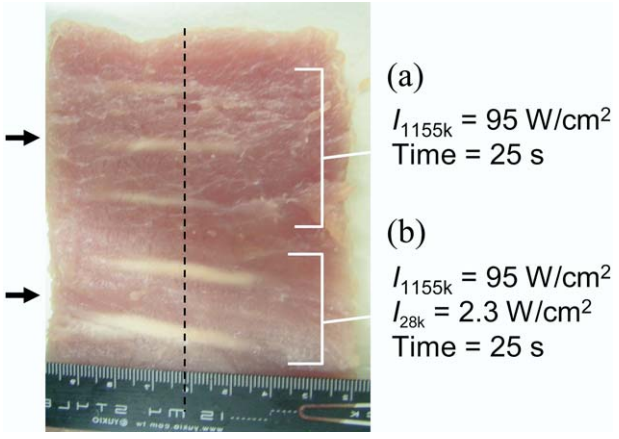

Fig. 6. Comparison of the thermal lesions generated in two conditions: (a) 95-W/cm^2, 1155-kHz ultrasound alone; and (b) combined 95-W/cm^2, 1155-kHz and 2.3-W/cm^2, 28-kHz ultrasound. In both cases the exposure time was 25 s. Vertical dashed line indicates the focal depth of the 566-kHz transducer.

Thermal Lesion Enlargement under Various Sonication Parameters

The enlargement of the thermal lesion by including low-frequency ultrasound under various sonication parameters was investigated next. The peak intensity of 566-/40-kHz ultrasound was set to 260/1.1 W/cm^2, and the exposure time ranged from 30 s to 100 s (with 10s increment). Figure 7 compares the lesion dimensions under arrangement 1 (566 and 40 kHz). Lesions formed during combined exposure to 40-kHz ultrasound were both wider and longer. Moreover, as the exposure time reached 70 s, the lesion enlargement along the axial direction tended to saturate to a similar dimension as that in the control group, whereas the lesion width continued to increase. Significant increases in the lesion length and width increase (as much as 140% and 200%) occurred for exposure times from 30 s to 50 s.

The thermal lesions formed with various sonication conditions in arrangement 2 (1155 and 28 kHz) were also investigated. Figure 8 compares the thermal lesion development for exposure times from 15 s to 45 s for 1155- and 28-kHz ultrasound at 95 and 2.3 W/cm^2, respectively. Significant increases in the lesion length and width (mean increases of 47% and 66%, respectively) occurred for intermediate exposure times from 25 s to 35 s. Lesion increase by using 95W/cm^2 in 35 s of exposure time was most apparent. For an exposure time of 15 s, the lesions appeared to be in an early development stage and the dimensions of the necrosed region did

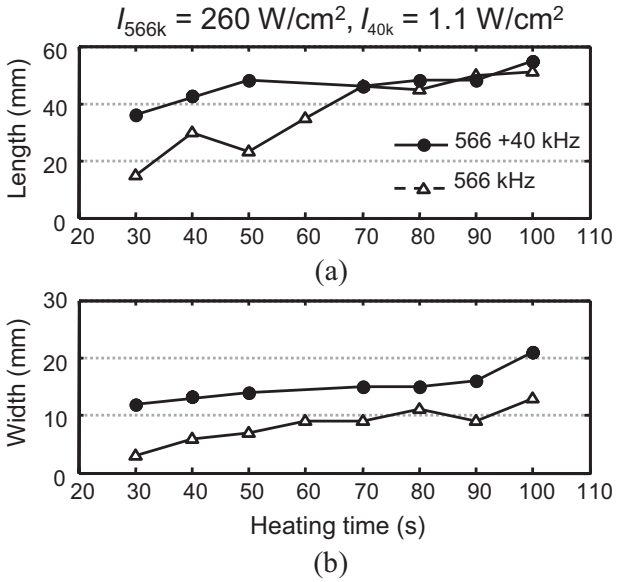

Fig. 7. Comparison of the thermal lesion dimensions in arrangement 1 between with and without the inclusion of 40-kHz ultrasound for exposure times from 30 to 100 s: (a) lesion length along the axial direction, and (b) lesion width along the radial direction. The peak intensities of the 566- and 40-kHz ultrasound were 260 and 1.1 W/cm^2, respectively.

not differ significantly from the distance from the focus and the lesion width ($p > 0.05$). For an exposure time of 45 s, the lesions had similar dimensions in the axial and radial directions, with no significant lesion shift from the focus ($p > 0.05$). A similar observation was made in arrangement 1 (Fig. 7(a)). Longer sonication times resulted in saturation of the necrosed volume that was limited by the dimensions of the samples used (data not shown).

Figure 9 compares the thermal lesions formed under three intensity/exposure-time combinations with and without 28-kHz ultrasound: 95 W/cm^2 for 35 s, 110 W/cm^2 for 25 s, and 125 W/cm^2 for 15 s. These parameters were selected because the resulting lesions could be easily observed. The thermal lesions were all enlarged in the presence of the low-frequency ultrasound, with mean increases in length and width as high as 39.6% and 60%; the enhancement was greatest at the lowest intensity and longest exposure time (*i.e.*, 95 W/cm^2 and 35 s).

Multiple Sonications to Generate a Large Thermal Lesion

Large thermal lesions can be created by moving the ultrasound transducer while sonicating the tissue (ter Haar 1995; Daum et al. 1999) The dynamics of the temperature build-up differ between the multiple- and single-sonication cases (Moros et al. 1990; Fan and Hynynen 1996). To ensure that the cavitation-enhanced heating can be used in multiple sonications, one-directional scan consisting of four 566-kHz ultrasound sonications were performed. Sonications were performed in three groups: (1) 566-kHz ultrasound alone (260 W/cm^2) for 40 or 80 s; (2) combined 566 kHz (260 W/cm^2) and 40 kHz (1.1 W/cm^2) for 40 s or 80 s; and (3) 566 kHz alone (450 W/cm^2) for 20 s or 40 s. The transducer spacing for adjacent sonications was 10 mm to provide sufficient gaps between lesions in group 1, and successive sonications were separated by 1 min to allow the temperature to decrease to <43°C (see Fig. 5(a) and (b)).

The necrotized areas induced in the three sonication groups are shown in Fig. 10. Comparison of groups 1 and 2 (Fig. 10(a) and (b)) reveals that introducing the low-frequency sonication resulted in a large increase in the necrosed volumes, with the gaps between the individual lesions being completely filled. Conversely, in group 3 (Fig. 10(c)) the adjacent four thermal lesions were connected at the anterior ends but not at the posterior ends. This is because each lesion tended to be tadpole shaped, with the

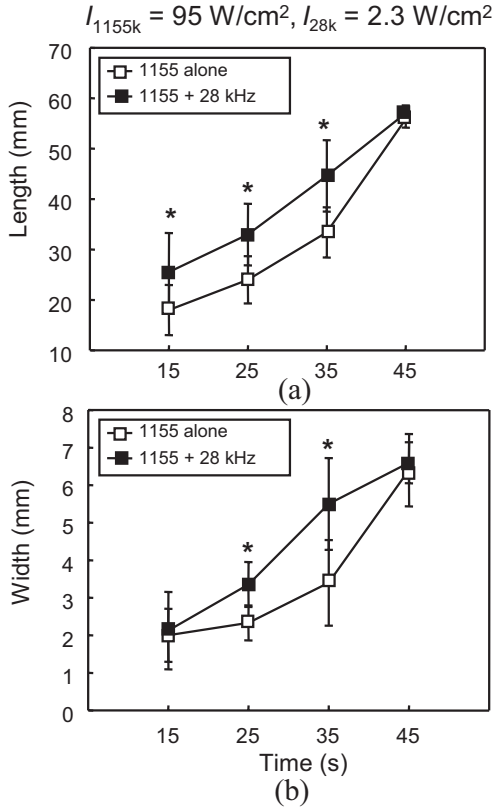

Fig. 8. Comparison of the thermal lesion dimensions (length and width) in arrangement 2 between with and without the inclusion of 40-kHz ultrasound for exposure times from 15 to 45 s. The peak intensities of the 566- and 28-kHz ultrasound were 95 and 2.3 W/cm^2, respectively. * indicates a statistical difference between the experimental and control groups ($p < 0.05$).

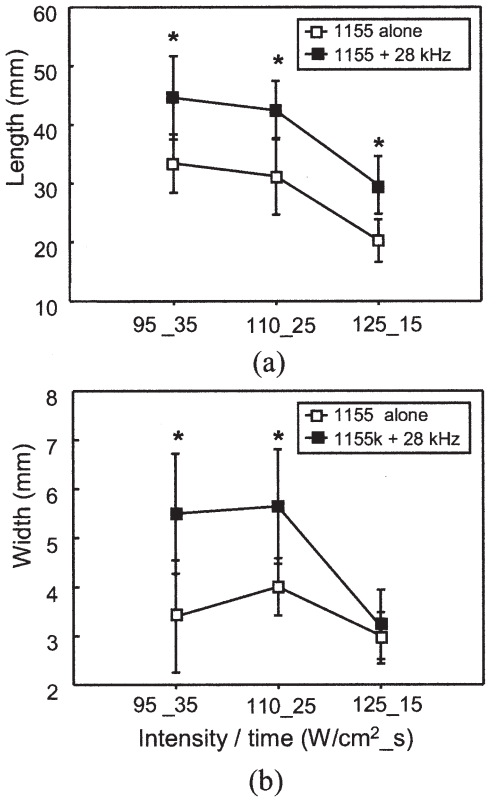

Fig. 9. Comparison of thermal lesion dimensions (length and width) in arrangement 2 between with and without the inclusion of 28-kHz ultrasound. The peak intensity of the 28-kHz ultrasound was constant at 2.3 W/cm^2, whereas that of the 1155-kHz ultrasound was 95, 110 and 125 W/cm^2 for exposure times of 35 s, 25 s and 15 s, respectively. * indicates a statistical difference between the experimental and control groups ($p < 0.05$).

adjacent lesions remaining open at the posterior ends and the necrosed area tending to shift toward the proximal end.

DISCUSSION

In this study, we investigated a novel cavitation-enhanced ultrasound heating based on combining high- and low-frequency ultrasound. Combining focused 566/1155 kHz with 40/28-kHz ultrasound increased the length and width of the formed lesions by as much as 140% and 200%, respectively, in arrangement 1 (566 and 40 kHz), and by as much as 47% and 66% in arrangement 2 (1155 and 28 kHz). Moreover, the use of ultrasound at two frequencies resulted in the thermal lesions maintaining a cigar shape and penetrating deeper, in contrast to the shallow tadpole-shaped or round lesions produced by existing cavitation-enhanced approaches (Chen et al. 2003; Sokka et al. 2003; Tran et al. 2003). Our approach was also able to induce smooth and well-connected lesions when using multiple sonications to generate larger and deeper thermal lesions, which could be especially beneficial in the generation of large and deep-seated thermal lesions.

Both of the arrangements used in the present study enlarged the thermal lesions, which suggests that the choice of low-frequency ultrasound is flexible. Second, the length/width ratio of the lesions did not appear to be affected by the addition of low-frequency ultrasound and maintained a similar value (calculated from Figs. 7, 8, and 9). This shows that the transducer's focal number (ratio of curvature radius to diameter) was still the key factor to determine the lesion's shape. The lesion enlargement was greater for combined 566- and 40-kHz ultrasound, but our experiments provide only limited data for determining the optimal frequencies; this should be investigated in future studies.

Acoustic cavitation enhanced by low-frequency ultrasound in the heating process can be identified by the occurrence of subharmonics and the increased emission of wideband-harmonics (Figs. 9 and 10). During the cavitation process, the expansion and oscillation of bubbles may increase the scattering of the transmitted wave, which also increases the ultrasound absorption, facilitates the temperature build-up and enlarges the resulting thermal lesion. This speculation is supported from the comparison of the temperatures elevations between single high-frequency sonication (see Fig. 4(a)) and com-

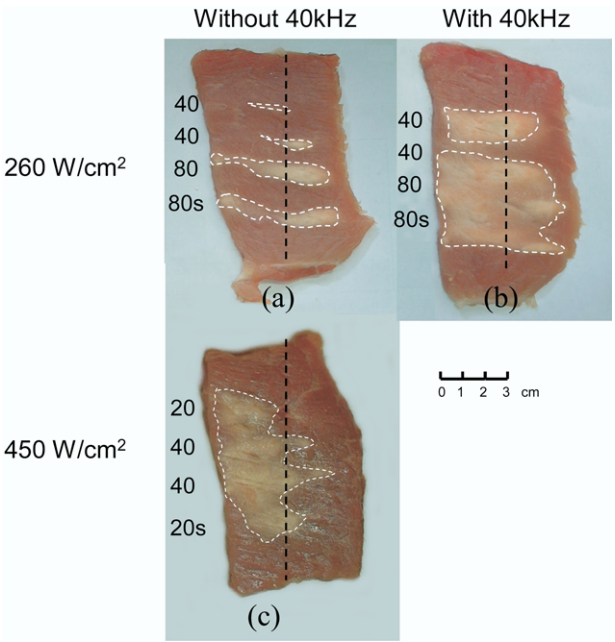

Fig. 10. One-dimensional scans for generating large thermal lesions: (a) 566-kHz ultrasound alone (260 W/cm^2) for 40 or 80 s, (b) combined 566 kHz (260 W/cm^2) and 40 kHz (1.1 W/cm^2) for 40 s or 80 s, and (c) 566 kHz (450 W/cm^2) for 20 s or 40 s.

bined high- and low-frequency sonication (see Fig. 4(b)). It also agrees with the prediction from a novel theoretical model by Chavrier et al. (2000), who showed that the attenuation coefficient was correlated with the concentration and radii of the bubbles.

The lesion shape in the present study differs from the conclusions of previous studies that tadpole-shaped lesions will be generated by using single-frequency focused ultrasound (Chen et al. 2003; Meaney et al. 2000; Sokka et al. 2003; Watkin et al. 1996). Strongly focused ultrasound with an intensity exceeding the cavitation threshold could, however, greatly increase the probability of bubble occurrence close to the focal point, with the resulting high concentration of bubbles aggregating to block ultrasound wave propagation through the focal plane and resulting in the boiling point being reached. This would lead to the development of an asymmetric lesion starting from the focal plane and extending toward the transducer. Meaney et al. (2000) employed a first-order approximation to model abnormal heat deposition distributions that accompanied high-ultrasound intensities, which successfully predicted shifts in thermal lesions as a result of bubble effects. Moreover, the theoretical model proposed by Chavrier et al. (2000) predicted that single high-frequency ultrasound of a high intensity (sufficient to produce cavitation) can induce a high concentration of bubbles in the near field that would act as a barrier to ultrasonic energy transmission, which contributes to tadpole-shaped lesions and lesions shifting toward the skin.

In contrast to ultrasound blocking by bubble aggregation and tissue boiling near the transducer focus, we speculated that the proposed low-frequency ultrasound induces cavitation-enhanced heating associated with evenly distributed bubbles in the tissue, which allows the ultrasound energy to propagate through the focal plane to induce more symmetrical thermal lesions. The effect could be important in preventing near-field heating during thermal treatments (Fan and Hynynen 1996; Liu et al. 2003).

Low-frequency ultrasound has been shown to produce biologic effects in mammal tissues, and has been extensively utilized to enhance sonophoresis, clot dissolution and fibrinolysis. The intensity used in low-frequency sonication is about an order of magnitude lower than that used in megahertz-frequency ultrasound (Terahara et al. 2002). Moreover, because of the low attenuation, deep penetration and long wavelength of low-frequency ultrasound, unwanted tissue damage can be induced outside the target area if too much energy is delivered. Possible damage includes cell destruction, and thermal- and cavitation-related damage. Ultrasound at intensities of 0.65 and 1.5 W/cm^2 enhances sonophoresis and drug-induced clot dissolution, respectively (Siegel et al. 2001; Suchkova et al. 1998). Moreover, Suchkova et al. (1998) showed that ultrasound at an intensity above 0.25 W/cm^2 for 1 h can accelerate fibrinolysis. Furthermore, 20-kHz ultrasound at about 6.5 W/cm^2 appears to result in cavitation (Tang et al. 2002), and 40-kHz ultrasound above 17 W/cm^2 thermally damages biologic tissue (Siegel et al. 2001). In the present study, the typical intensities of the 40- and 28-kHz ultrasound in arrangements 1 and 2 were 1.1 and 2.3 W/cm^2, respectively. The intensity levels of the low-frequency ultrasound applied in the present could, therefore, induce ultrasound bioeffects, but were sufficiently low enough to avoid unwanted cavitation and thermal-related damage outside the treatment region. Although there is no definitive report that the intensity levels we used could destroy cell membranes in transdermal usage, low-frequency ultrasound still contains potential dangers and might cause gradual bubble generation in normal tissue and blood vessels, and should be therefore avoided (Crum and Mao 1996). To avoid overexposing surrounding tissue to low-frequency ultrasound, multiple transducers can be arranged as overlapping energy sources to improve the intensity uniformity at the target portion while reducing the possibility of overexposure in the surrounding normal tissues.

Introducing low-frequency ultrasound into focused ultrasound thermal therapy represents an alternative to the cavitation-enhanced ultrasound thermal ablation. Enhancing the thermal heating effects by low-frequency sonication provides unique features compared with other modalities such as ultrasound contrast agents (Tran et al. 2003) and high-power-burst presonication (Sokka et al. 2003). For example, biologic tissues absorb less low-frequency ultrasound (compared with megahertz-frequency ultrasound), which can reduce heating of the rib or skull during transrib or transcranial treatment. However, the relative long wavelength of ultrasound at hundreds of kilohertz frequencies (for example, 37.5 mm in 40 kHz) makes it difficult to generate localized constructive interference at a millimeter level. This can be improved by using multiple low-frequency ultrasound transducers to provide energy superimposition around the geometrical center of the transducer array.

This study has verified the cavitation-enhanced heating introduced by combined low- and high-frequency sonication in *ex vivo* tissues, but the extrapolation to *in vivo* tissue needs to be considered. Tang et al. (2002b) experimentally verified that acoustic cavitation is the major factor in low-frequency–induced skin permeability. They used a number of types of *in vitro* skin and *in vivo* pig skin to investigate the correlation of *in vivo*/*in vitro* tissue permeability during low-frequency sonophoresis (Tang et al. 2002a); they found that living skin was more sensitive to ultrasound treatment than excised skin. Hence, the sonication parameters used in *ex vivo* tissue were sufficient to induce the same degree of skin permeabilization in *in vivo* tissue. On the other hand, Melodelima et al. (2004) proposed that using high-intensity short-duration presonication (60 W/cm^2) before the normal heating process (at 14

W/cm^2) with a planar transducer can induce cavitation-enhanced heating in *ex vivo* tissue. Goldenstedt et al. (2004) re-examined the same treatment protocol *in vivo*, and concluded that the intensity of the short-duration presonication was identical, yet a higher intensity for the subsequent heating was required (increased from 14 to 30 W/cm^2). This may be the result of ultrasonic energy dissipation caused by blood perfusion and circulation. Hence, when applying the method described in the present study *in vivo*, the intensity of the low-frequency ultrasound reported here may be sufficient to provide acoustic cavitation, whereas the intensity of the high-frequency ultrasound may need to be increased to compensate for the energy losses due to the blood perfusion. Moreover, the heating-energy difference in the tissue temperature between this study (25°C) and *in vivo* (37°C) may also need to be considered.

CONCLUSION

This study demonstrates the feasibility and efficacy of implementing cavitation-enhanced thermal heating by combining megahertz- and kilohertz-frequency ultrasound. The cavitation threshold is lower for low-frequency ultrasound, which makes it easier to induce cavitation and thereby can enhance the thermal heating induced by high-frequency ultrasound. The generated lesions were more symmetrical and less shifted, implying that deeper portions can be treated. This property is also advantageous in improving the uniformity of large thermal lesions produced by scanning the ultrasound transducer. This study provides useful data for cavitation-enhanced heating, and may also provide the basis for exploring new applications of low-frequency ultrasound.

REFERENCES

Atchley AA, Crum LA. Acoustic cavitation and bubble dynamics. In: Suslick KS, ed. Ultrasound. Its chemical, physical, and biologic effects. New York: VCH Publishers, 1988:1–64.

Barnett SB. Ultrasound. Nonthermal issues: Cavitation—Its nature, detection and measurement. Ultrasound Med Biol 1998;24 Suppl 1:S11–21.

Chapelon JY, Ribault M, Vernier F, Souchon R, Gelet A. Treatment of localised prostate cancer with transrectal high intensity focused ultrasound. Eur J Ultrasound 1999;9:31–38.

Chen WS, Lafon C, Matula TJ, Vaezy S, Crum LA. Mechanisms of lesion formation in high intensity focused ultrasound therapy. Acoust Res Lett Online 2003;4:41–46.

Crum LA, Mao Y. Acoustically enhanced bubble growth at low frequencies and its implications for human diver and marine mammal safety. J Acoust Soc Am 1996;99:2898–2907.

Damianou C, Hynynen K. Focal spacing and near-field heating during pulsed high temperature ultrasound therapy. Ultrasound Med Biol 1993;19:777–787.

Daum DR, Smith NB, King R, Hynynen K. In vivo demonstration of noninvasive thermal surgery of the liver and kidney using an ultrasonic phased array. Ultrasound Med Biol 1999;25:1087–1098.

Fan X, Hynynen K. Ultrasound surgery using multiple sonications—Treatment time considerations. Ultrasound Med Biol 1996;22:471–482.

Flynn HG. Generation of transient cavities in liquids by microsecond pulses of ultrasound. J Acoust Soc Am 1982;72:1926–1932.

Fry FJ, Kossoff G, Eggleton RC, Dunn F. Threshold ultrasonic dosages for structural changes in the mammalian brain. J Acoust Soc Am 1970;48:1413–1417.

Goldenstedt C, Melodelima D, Mithieux F, Chesnais S, Theillere Y, Cathignol D. Cavitation enhances treatment depth when combined with thermal effect using a plane ultrasound transducer: an in vivo study. IEEE Ultrason Symp 2004;1:709–712.

Hynynen K. The threshold for thermally significant cavitation in dog's thigh muscle in vivo. Ultrasound Med Biol 1991;17:157–169.

Hynynen K, Darkazanli A, Unger E, Schenck JF. MRI-guided noninvasive ultrasound surgery. Med Phys 1993;20:107–115.

Lele PP, Parker KJ. Temperature distributions in tissues during local hyperthermia by stationary or steered beams of unfocused or focused ultrasound. Br J Cancer Suppl 1982;45:108–121.

Liu HL, Chen YY, Yen JY, Lin WL. Treatment time reduction for large thermal lesions by using a multiple 1D ultrasound phased array system. Phys Med Biol 2003;48:1173–1190.

Meaney PM, Cahill MD, ter Haar GR. The intensity dependence of lesion position shift during focused ultrasound surgery. Ultrasound Med Biol 2000;26:441–450.

Melodelima D, Chapelon JY, Theillere Y, Cathignol D. Combination of thermal and cavitation effects to generate deep lesions with an endocavitary applicator using a plane transducer: Ex vivo studies. Ultrasound Med Biol 2004;30:103–111.

Moros EG, Roemer RB, Hynynen K. Pre-focal plane high-temperature regions induced by scanning focused ultrasound beams. Int J Hyperthermia 1990;6:351–366.

Nyborg WL. Heat generation by ultrasound in a relaxing medium. J Acoust Soc Am 1981;70:310–312.

Sanghvi NT, Hawes RH. High-intensity focused ultrasound. Gastrointest Endosc Clin North Am 1994;4:383–395.

Siegel RJ, Atar S, Fishbein MC, et al. Noninvasive transcutaneous low frequency ultrasound enhances thrombolysis in peripheral and coronary arteries. Echocardiography 2001;18:247–257.

Sokka SD, King R, Hynynen K. MRI-guided gas bubble enhanced ultrasound heating in in vivo rabbit thigh. Phys Med Biol 2003;48:223–241.

Suchkova V, Siddiqi FN, Carstensen EL, Dalecki D, Child S, Francis CW. Enhancement of fibrinolysis with 40-kHz ultrasound. Circulation 1998;98:1030–1035.

Tang H, Blankschtein D, Langer R. Effects of low-frequency ultrasound on the transdermal permeation of mannitol: Comparative studies with in vivo and in skin. J Pharm Sci 2002a;91:1776–1794.

Tang H, Wang CC, Blankschtein D, Langer R. An investigation of the role of cavitation in low-frequency ultrasound-mediated transdermal drug transport. Pharm Res 2002b;19:1160–1169.

ter Haar G. Ultrasound focal beam surgery. Ultrasound Med Biol 1995;21:1089–1100.

Terahara T, Mitragotri S, Kost J, Langer R. Dependence of low-frequency sonophoresis on ultrasound parameters; distance of the horn and intensity. Int J Pharm 2002;235:35–42.

Tran BC, Seo J, Hall TL, Fowlkes JB, Cain CA. Microbubble-enhanced cavitation for noninvasive ultrasound surgery. IEEE Trans Ultrason Ferroelectr Freq Control 2003;50:1296–1304.

Vaezy S, Martin R, Yaziji H, et al. Hemostasis of punctured blood vessels using high-intensity focused ultrasound. Ultrasound Med Biol 1998;24:903–910.

Vallancien G, Chartier-Kastler E, Harouni M, Chopin D, Bougaran J. Focused extracorporeal pyrotherapy: experimental study and feasibility in man. Semin Urol 1993;11:7–9.

Vykhodtseva NI, Hynynen K, Damianou C. Histologic effects of high intensity pulsed ultrasound exposure with subharmonic emission in rabbit brain in vivo. Ultrasound Med Biol 1995;21:969–979.

Watkin NA, ter Haar GR, Rivens I. The intensity dependence of the site of maximal energy deposition in focused ultrasound surgery. Ultrasound Med Biol 1996;22:483–491.

Wu F, Chen WZ, Bai J, et al. Pathological changes in human malignant carcinoma treated with high-intensity focused ultrasound. Ultrasound Med Biol 2001;7:1099–1106.